BIOCHEMISTRY
including biophysical chemistry & molecular biology

Article

pubs.acs.org/biochemistry

Mechanistic Basis for the Potent Anti-Angiogenic Activity of Semaphorin 3F

Hou-Fu Guo,[†] Xiaobo Li,[†] Matthew W. Parker,[†] Johannes Waltenberger,[‡] Patrice M. Becker,[§,∥] and Craig W. Vander Kooi*[,†]

[†]Department of Molecular and Cellular Biochemistry, Center for Structural Biology, University of Kentucky, Lexington, Kentucky 40536, United States

[‡]Division of Cardiology, Department of Cardiovascular Medicine, University Hospital Münster, 48149 Münster, Germany

[§]Division of Pulmonary and Critical Care Medicine, Johns Hopkins University School of Medicine, Baltimore, Maryland 21205, United States

ABSTRACT: Neuropilin-1 (Nrp1), an essential type I transmembrane receptor, binds two secreted ligand families, vascular endothelial growth factor (VEGF) and class III Semaphorin (Sema3). VEGF-A and Sema3F have opposing roles in regulating Nrp1 vascular function in angiogenesis. VEGF-A functions as one of the most potent pro-angiogenic cytokines, while Sema3F is a uniquely potent endogenous angiogenesis inhibitor. Sema3 family members require proteolytic processing by furin to allow competitive binding to Nrp1. We demonstrate that the furin-processed C-terminal domain of Sema3F (C-furSema) potently inhibits VEGF-A-dependent activation of endothelial cells. We find that this potent activity is due to unique heterobivalent engagement of Nrp1 by two distinct sites in the C-terminal domain of Sema3F. One of the sites is the C-terminal arginine, liberated by furin cleavage, and the other is a novel upstream helical motif centered on the intermolecular disulfide. Using a novel chimeric C-furSema, we demonstrate that combining a single C-terminal arginine with the helical motif is necessary and sufficient for potent inhibition of binding of VEGF-A to Nrp1. We further demonstrate that the multiple furin-processed variants of Sema3A, with the altered proximity of the two binding motifs, have dramatically different potencies. This suggests that furin processing not only switches Sema3 to an activated form but also, depending on the site processed, can also tune potency. These data establish the basis for potent competitive binding of Sema3 to Nrp1 and provide a basis for the design of bivalent Nrp inhibitors.

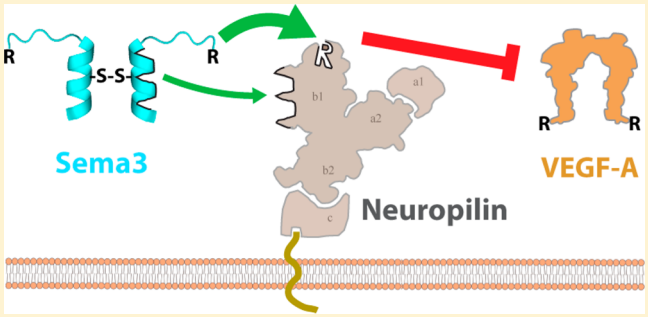

Neuropilins (Nrps) make up an essential cell surface receptor family.[1] They function with vascular endothelial growth factor receptors (VEGFRs) in VEGF-dependent angiogenesis and with Plexin receptors in Sema3-dependent axon guidance.[2−6] In addition to their function in neurons, a critical role for specific Sema3 family members in physiological and pathological regulation of the cardiovascular system has been increasingly recognized.[7−9] For example, Sema3F is critical for maintaining an avascular outer retina, while Sema3A and Sema3E have important roles in vascular patterning.[9−12] In contrast, mutation and downregulation of Sema3 family members are also observed in many types of solid tumors and have been directly correlated with tumor angiogenesis and cancer progression.[7,13,14] Indeed, restoring the expression of Sema3B and Sema3F in tumors inhibits further cancer progression *in vitro* and *in vivo*.[15−18]

Nrp serves a central role in integrating the opposing signals of VEGF and Sema3 in both physiological and pathological contexts through competitive ligand binding. The Nrp1-b1 coagulation factor domain has a conserved C-terminal arginine binding pocket that is critical for competitive VEGF and Sema3 binding.[19,20] Alternative splicing of VEGF-A regulates Nrp1 binding,[21] with the exon 8-encoded C-terminal arginine residue being necessary for binding Nrp1-b1.[22] In contrast, furin proteolysis of Sema3 is critical for regulating its ability to bind Nrp and function. Furin processing can either inactivate or activate Sema3 by processing at sites in the central or C-terminal domains, respectively. Processing in the central region of Sema3 has been primarily reported to inactivate Sema3 activity by cleaving the protein into two fragments, although the fragments may still possess activity.[23−25] Furin processing within the Sema3 C-terminal domain is critical to activate the Sema3 pro-protein by producing a C-terminal arginine, allowing competitive engagement of Nrp1-b1.[20,26]

Multiple C-terminal arginine-containing peptides and peptido-mimetics have been produced as competitive antagonists of VEGF-A−Nrp1 binding.[27−29] While these peptides function as inhibitors *in vitro* and *in situ*, their efficacy and that

Received: July 31, 2013
Revised: September 30, 2013
Published: September 30, 2013

   dx.doi.org/10.1021/bi401034q | *Biochemistry* 2013, 52, 7551−7558

of peptido-mimetics suffer from limited potency ($IC_{50} \approx 10-50$ μM). In contrast, endogenous Sema3F functions as a potent inhibitor of binding of VEGF-A to Nrp1.[20] However, the molecular mechanism of high-affinity binding of Sema3F to Nrp1 has not been elucidated, leaving open the question of how Sema3F potently competes for Nrp1 binding.

In this study, we demonstrate the mechanistic basis for the potency of the furin-processed C-terminal domain of Sema3F (C-furSema) (Figure 1A) *in vitro* and *in situ*. We find that C-furSema exhibits unique heterobivalent engagement of Nrp1 that is essential for high-affinity binding. Further, different C-terminal furin-processed Sema3A isoforms show a range of potencies, which correlates with the distance between the helical and C-terminal arginine binding motifs.

EXPERIMENTAL PROCEDURES

C-furSema and Variant Production. Homodimeric C-furSema (GLIHQYCQGYWRHVPPSPREAPGAPRSPEPDQ-KKPRNRR), truncations, and point mutants were synthesized using solid phase synthesis, oxidized to produce the natural intermolecular disulfide, and purified via reversed phase high-performance liquid chromatography (HPLC) using a 4.6 mm × 250 mm, SinoChrom ODS-BP column to >95% purity (Neo-Peptide, Cambridge, MA). The monomeric C-furSema^{Mon} (GLIHQYSQGYWRHVPPSPREAPGAPRSPEPDQKKPRN-RR) was produced in the same manner without oxidization. C-furSema^{Het} was produced by combining separately synthesized reduced C-furSema and C-furSema^{Helix} (GLIHQYCQGYW-RH), oxidized in the presence of the excess C-furSema^{Helix}, and purified via reversed phase HPLC using a 4.6 mm × 250 mm, SinoChrom ODS-BP column to >95% purity (LifeTein, South Plainfield, NJ). All C-furSema variants were well behaved in solution and soluble to >1 mM. A dimeric construct of C-furSema^{Helix} alone showed limited solubility, with a maximal solubility in phosphate-buffered saline (PBS) of 20 μM, and no ability to inhibit VEGF-A binding up to the limit of solubility.

Protein and peptide concentrations were determined using OD_{280} values measured on a Nanodrop 1000 (Thermo Fisher Scientific, Wilmington, DE).

***In Situ* Inhibition Assays.** Porcine aortic endothelial (PAE) cells stably overexpressing VEGFR-2 and Nrp1 were utilized to measure the ability of C-furSema to block VEGF-A activation of VEGFR-2.[30] PAE cells were grown in F12 medium (Invitrogen, Grand Island, NY) supplemented with 10% fetal bovine serum (FBS) (Invitrogen) and 1% Pen/Strep in six-well cell culture plates to 70% confluence. Cells were then serum-starved for 16 h in Endothelial cell basal growth medium-2 (EBM-2) (Lonza, Walkersville, MD). C-furSema samples were resuspended in EBM-2, added at a final concentration of 10 μM, and incubated for 90 min at 37 °C. Cells were then stimulated with 100 ng/mL VEGF-A (R&D Systems, Minneapolis, MN) for 3 min. After 3 min, the medium was removed and cells were solubilized in RIPA buffer supplemented with phosphatase and protease inhibitor (Roche). Total VEGFR-2 and VEGFR-2 phosphorylation were determined by Western blotting using 55B11 and 19A10 antibodies (Cell Signaling, Danvers, MA), respectively, at a 1:1000 dilution followed by a goat anti-rabbit horseradish peroxidase (HRP)-conjugated secondary antibody at 1:20000 dilution (sc-2301, Santa Cruz). The SuperSignal West Femto chemiluminescence (ECL) detection system (Thermo Fisher Scientific, Rockford, IL) was used for detection of immunoreactivity on X-ray films (HyBlot CL, Denville Scientific, Inc., Metuchen, NJ). Experiments were performed in triplicate, and results are reported as means ± the standard deviation.

For the determination of *in situ* potency, a VEGFR-2 cellular phosphorylation sandwich enzyme-linked immunosorbent assay (ELISA) was utilized (ProQinase). Primary human umbilical vein endothelial cells (HUVECs) were plated in endothelial cell growth medium (ECGM) supplemented with 10% FBS (PromoCell), serum-starved for 16 h, incubated with varying concentrations of C-furSema for 90 min, and then activated with VEGF-A at a concentration of 100 ng/mL for 3 min. The level of VEGFR-2 phosphorylation was determined via a sandwich ELISA using a VEGFR-2 capture antibody and an anti-phosphotyrosine detection antibody (PromoCell). Raw data were converted into percent phosphorylation relative to high and low controls. Cells treated with VEGF-A alone were defined as high control (100%), and those treated with 1 μM sunitinib, a well-characterized VEGFR-2 kinase inhibitor with an IC_{50} of 10 nM, were defined as low control (0%). Inhibition curves were fit using a standard four-parameter sigmoidal curve to yield the IC_{50}. Experiments were performed in duplicate, and results are reported as means ± the standard deviation.

Protein Expression and Purification. Proteins were expressed and purified using established protocols.[20] Briefly, Nrp1-b1b2 (residues 274−586) was expressed in *Escherichia coli* and purified using nickel affinity chromatography (IMAC) followed by heparin affinity chromatography. Alkaline phosphatase (AP)-fused VEGF-A was produced from Chinese hamster ovary (CHO) cells.

***In Vitro* Inhibition Assays.** Plate-based inhibition assays were performed as previously reported.[20] Briefly, 410 μM *p*-nitrophenol phosphate (pNPP) hydrolyzed per minute per microliter of AP-VEGF-A was combined with Sema3F-derived peptides in binding buffer [20 mM Tris (pH 7.5) and 50 mM NaCl], incubated with Nrp1 affinity plates for 1 h at 25 °C, washed three times with PBS-T [0.01 M phosphate-buffered saline and 0.1% Tween 20 (pH 7.4)], incubated with PBS-T for 5 min, aspirated, and developed by addition of 100 μL of 1× alkaline phosphatase pNPP substrate[31] followed by quenching with 100 μL of 0.5 N NaOH. AP activity was quantitatively measured at 405 nm using a SpectraMax M5 instrument (Molecular Devices, Sunnyvale, CA). Binding curves were fit using a standard four-parameter sigmoidal curve to yield the IC_{50}. Inhibitory potency is expressed per subunit for peptides to allow direct comparison between dimeric and monomeric peptides. Experiments were performed in triplicate, and results are reported as means ± the standard deviation. An unpaired *t* test was used to compare IC_{50} values.

Circular Dichroism (CD). C-furSema and C-furSema^{Mon} were dissolved in 0.01 M sodium phosphate and 50 mM NaCl (pH 6.5) at a concentration of 0.5 mg/mL. CD spectra were measured using a J-810 spectrapolarimeter (Jasco, Easton, MD) with a 1 mm path length quartz cuvette. All measurements were performed at 25 °C and three scans averaged for each spectrum. A blank spectrum was collected in the same manner and used for background subtraction. The fraction of secondary structure was determined by K2D3 using the wavelength range of 200−240 nm.[32]

RESULTS

C-furSema Is a Potent Inhibitor *in Situ*. To determine the potency of C-furSema function in a cellular context, we examined its ability to inhibit VEGF-A-mediated activation of VEGFR-2. Nrp1 and VEGFR-2 were stably expressed in PAE

dx.doi.org/10.1021/bi401034q | *Biochemistry* 2013, 52, 7551−7558

cells,[30] and the ability of C-furSema to inhibit VEGF-A-dependent phosphorylation of VEGFR-2 Y1175 was assessed. C-furSema markedly inhibited VEGF-A-dependent VEGFR-2 activation (Figure 1B). To confirm this finding in a distinct cell type and determine the potency and extent of this inhibition in primary endothelial cells, we measured the dose-dependent inhibitory effect of C-furSema on the activation of VEGFR-2 in HUVECs using a quantitative sandwich ELISA. Strikingly, C-furSema showed potent inhibition of VEGFR-2 activation with an IC_{50} of 34 ± 15 nM (Figure 1C), consistent with its potency *in vitro*,[20] and more than 2 orders of magnitude greater than those of short peptide inhibitors of Nrp1.[27,28,33,34] Additionally, complete inhibition of VEGFR-2 activation was observed in HUVECs, in contrast to other Nrp inhibitors that are able to only partially inhibit VEGFR-2 activation even at their maximal dose.[28] Thus, C-furSema is a potent inhibitor of Nrp1-dependent activation of endothelial cells *in situ*.

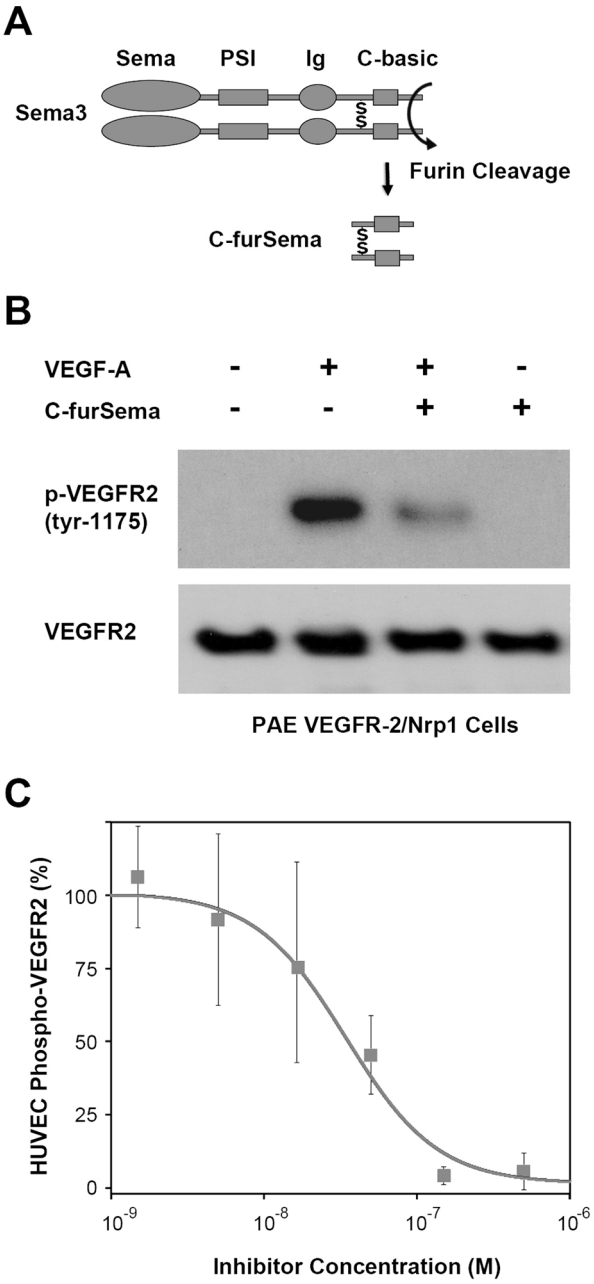

Figure 1. C-furSema potently inhibits VEGF-A-mediated VEGFR-2 activation *in situ*. (A) Schematic representation of Sema3 highlighting the furin-processed C-terminal domain (C-furSema). (B) Activation of PAE cells stably overexpressing Nrp1 and VEGFR-2 by VEGF-A is inhibited by C-furSema as demonstrated by a decrease in the level of autophosphorylation of Tyr-1175 of VEGFR-2. (C) C-furSema is a potent, dose-dependent inhibitor of VEGF-A-mediated HUVEC activation as demonstrated by a sandwich ELISA (IC_{50} = 34 ± 15 nM). Phospho-VEGFR-2 levels were normalized to VEGF-A alone and 1 μM sunitinib.

Mechanism of C-furSema Potency. C-furSema, which corresponds to the full C-terminal basic domain of Sema3F, is larger and more complex than peptide and peptido-mimetic inhibitors that have been developed to target Nrp1. Given the dimeric nature of C-furSema, because of its conserved intermolecular disulfide bond, we predicted that the potency of C-furSema might be attributable to avidity effects arising from the dual engagement of Nrp1. Indeed, previous studies have demonstrated that oligomeric peptide inhibitors of Nrp have enhanced potency.[28]

To test this, we produced a monomeric form of C-furSema by mutating the single conserved cysteine residue responsible for dimerization to serine (C-furSema^{Mon}). The ability of C-furSema and C-furSema^{Mon} to competitively block binding of VEGF-A to Nrp1 was compared (Figure 2). A significant decrease in potency was observed for the monomer (black line; IC_{50} = 1.3 ± 0.7 μM) compared to the dimer (gray line; IC_{50} = 24 ± 1 nM). While these data indicate a direct correlation of oligomerization and potency, it is notable that the monomeric species of C-furSema is still an order of magnitude more potent than previously published inhibitors,[27,28,33,34] suggesting that additional mechanisms may contribute to C-furSema potency.

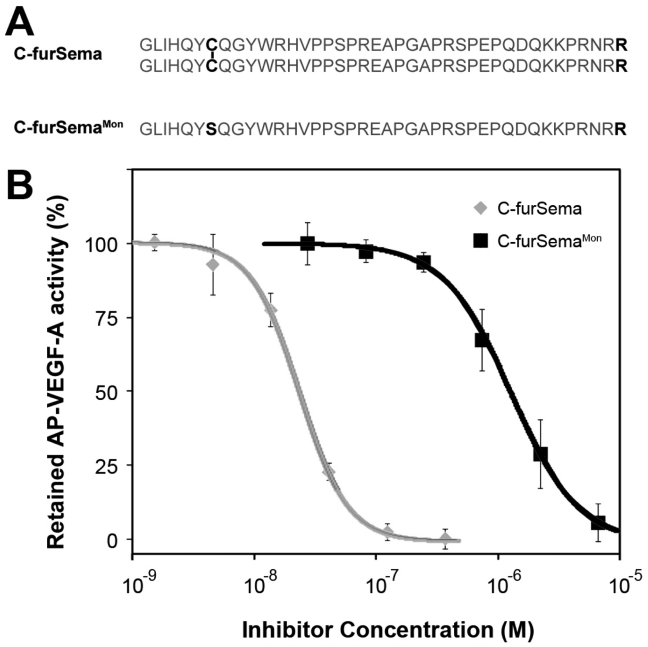

Figure 2. Effect of the intermolecular disulfide on C-furSema potency. (A) Comparison of dimeric C-furSema and C-furSema^{Mon}. (B) Critical role for the conserved intermolecular disulfide C-furSema (gray line; IC_{50} = 24 ± 1 nM) and C-furSema^{Mon} (black line; IC_{50} = 1.3 ± 0.7 μM) in inhibiting binding of VEGF-A to Nrp1.

A C-terminal arginine has been shown to be critical for Nrp ligand binding.[19] In the Sema3 family, furin processing liberates

dx.doi.org/10.1021/bi401034q | *Biochemistry* 2013, 52, 7551−7558

a C-terminal arginine and is required for Nrp binding.[20,26] In Nrp1 ligands, residues near the C-terminal arginine have been shown to contribute to potency and selectivity.[22,35] Thus, we hypothesized that residues directly upstream of the C-terminus might be responsible for enhanced potency.

To test the role of the C-terminal residues, we performed alanine scanning mutagenesis of the seven C-terminal residues of C-furSema (Figure 3A,B). As expected, mutation of the C-terminal arginine of C-furSema to alanine, R779A, dramatically decreased its inhibition potency by greater than two orders of magnitude (IC_{50} = 4.5 ± 0.2 μM). Surprisingly, no other mutation decreased the C-furSema potency. In fact, the R778A was slightly more potent, consistent with a recent report of a role for the C-1 position in tuning potency.[35] These data confirm the importance of a C-terminal arginine in binding of Sema3 to Nrp1 but indicate that the residues directly upstream minimally contribute to potent competitive binding to Nrp1. Therefore, the enhanced potency of C-furSema relative to other peptide inhibitors cannot be explained by additional interactions within the region directly proximal to the C-terminal arginine.

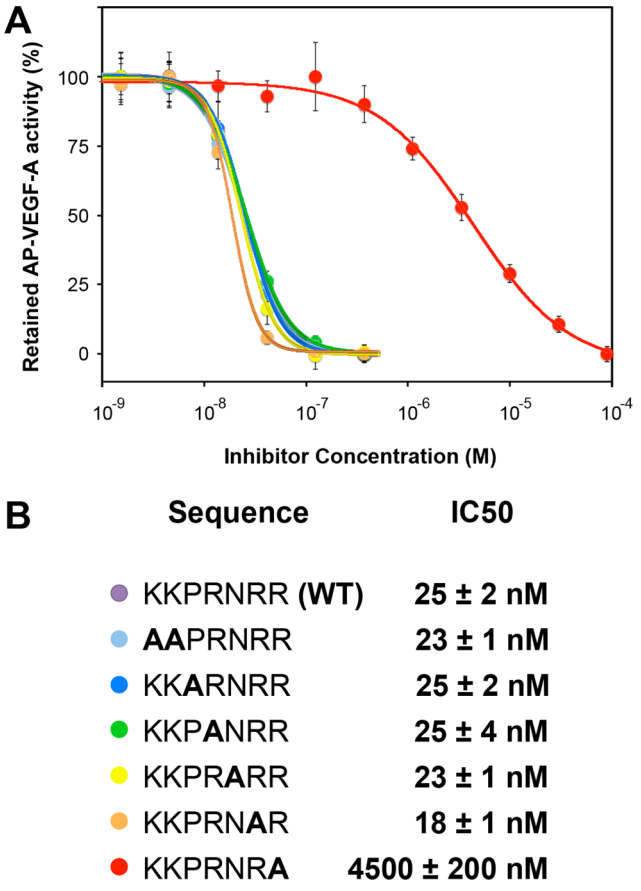

Figure 3. C-furSema C-terminal arginine contributes to high-affinity binding to Nrp. (A) An alanine scan of the C-terminus of C-furSema was performed. The ability of C-furSema and mutants to inhibit AP-VEGF-A binding to Nrp1 was determined. (B) Inhibition curves were utilized to determine peptide potency (IC_{50}), with a significant decrease only observed with the C-terminal arginine mutant.

Contribution of the N-Terminal Helical Region. In addition to the C-terminus, the N-terminal sequence of C-furSema is conserved across species. Furthermore, secondary structure predictions indicate α-helical propensity for the 11 amino acids centered around the cysteine (Figure 4A). Notably, this is the only predicted structured region in the otherwise extended C-terminal basic domain of Sema3. On the basis of this, we hypothesized that the N-terminus may be involved in binding to Nrp1. To test this, we produced a protein with half of the predicted helix deleted but that retained the conserved cysteine residue necessary and sufficient for dimerization (ΔN-C-furSema). On the basis of a simple avidity model, ΔN-C-furSema should have unaltered inhibitory potency. Strikingly, ΔN-C-furSema was approximately 5-fold less potent (IC_{50} = 111 ± 21 nM) than C-furSema (IC_{50} = 25 ± 3 nM) (Figure 4B). These data suggest that the N-terminal region of C-furSema, centered around the conserved cysteine, contributes to the potent competitive inhibition of binding of VEGF-A to Nrp1. However, this could be due to either direct binding of

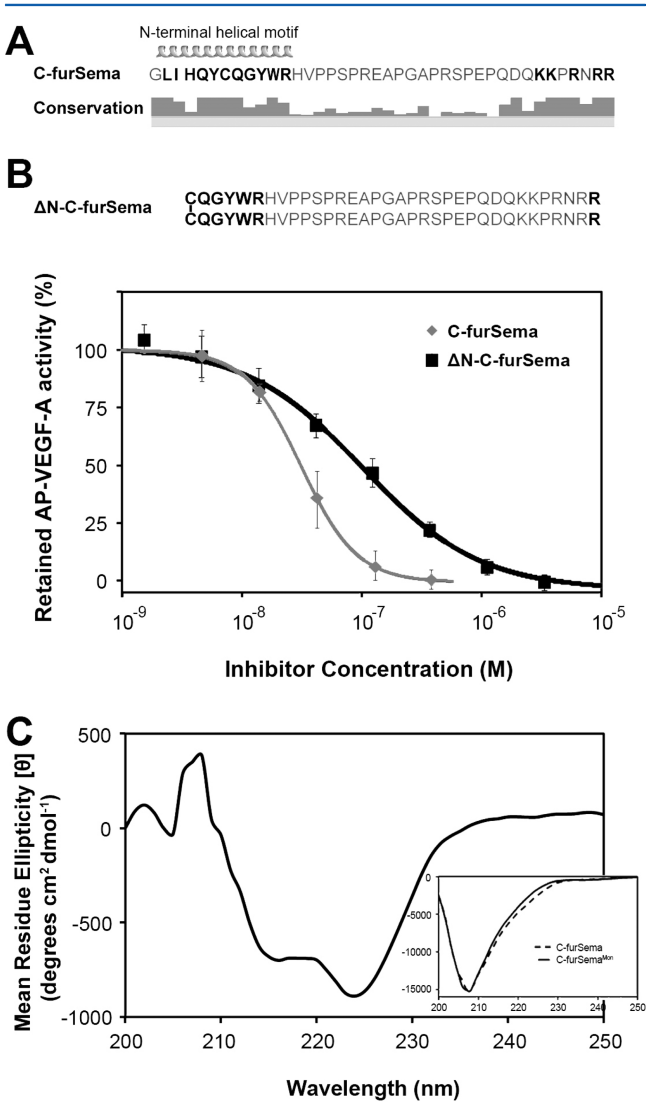

Figure 4. N-Terminal helical motif is a structured region that contributes to potency. (A) Sequence, predicted secondary structure, and conservation of C-furSema (based on an alignment of human, rat, mouse, cow, dog, chicken, and zebrafish orthologs). (B) ΔN-C-furSema, an N-terminal helical deletion, decreases the potency of C-furSema (IC_{50} values of 111 ± 21 and 25 ± 3 nM, respectively). (C) Difference CD spectrum of dimeric vs monomeric C-furSema reveals a characteristic loss of α-helical content. The inset shows CD spectra of dimeric C-furSema (---) and C-furSema^{Mon} (—).

dx.doi.org/10.1021/bi401034q | Biochemistry 2013, 52, 7551−7558

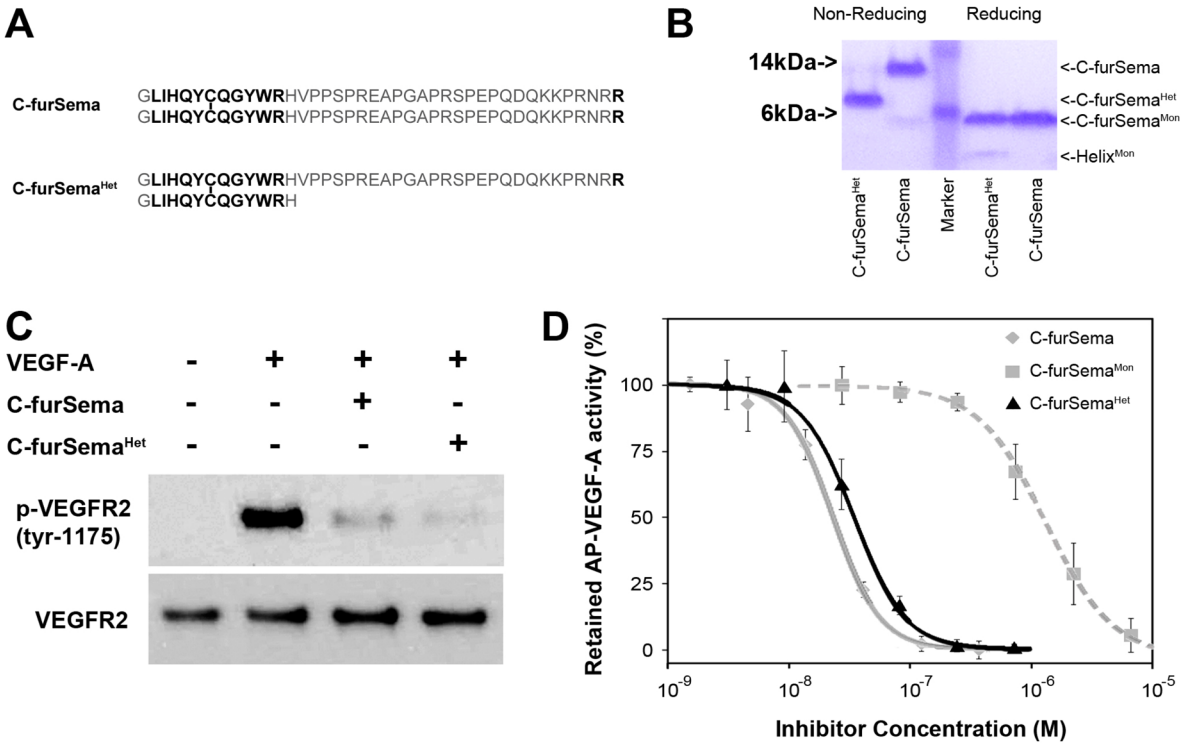

Figure 5. Helical motif determines potent competitive Nrp1 binding. (A) To determine the contribution of the N-terminal helical region to mediating Nrp inhibition, C-furSema^{Het} was synthesized. (B) Comparison of nonreducing vs reducing SDS−PAGE demonstrates the purity and correct intermolecular disulfide bond formation of C-furSema and C-furSema^{Het}. (C) C-furSema and C-furSema^{Het} equivalently inhibit VEGF-A-dependent activation of PAE cells and (D) have nearly equal potencies (IC_{50} values of 24 ± 1 and 35 ± 3 nM, respectively).

the N-terminal region to Nrp1 or indirect effects of orienting the two C-terminal arginines for optimal Nrp binding.

The conserved cysteine of C-furSema is required both for oligomerization and for potent competitive Nrp1 binding. Interestingly, the cysteine is centered within the predicted N-terminal helix. This led us to examine the possibility of an additional role for the intermolecular disulfide in maintaining the structure of the N-terminal region. Thus, we compared the secondary structure of C-furSema and C-furSema^{Mon} using CD. The overall spectra are consistent with the predicted secondary structure of C-furSema, an overall coil with a smaller helical component. The difference spectrum clearly shows a loss of helical character in C-furSema^{Mon} (Figure 4C). Fitting the individual spectra reveals an approximately 30% loss of helicity in C-furSema^{Mon}, with a 16% overall helical composition for C-furSema compared to 11% for C-furSema^{Mon}. These data indicate that the conserved cysteine that forms the key intermolecular disulfide in Sema3F is important not only for determining the oligomeric state of C-furSema but also for stabilizing the N-terminal helical region of C-furSema required for potent engagement of Nrp1.

We interpret these data to indicate that the disulfide-stabilized N-terminal helix directly contributes to Nrp1 binding. However, it remains possible that this region indirectly affects potency by imposing conformational constraints that orient the C-furSema dimer. To distinguish between these possibilities, we designed a heterodimer composed of one subunit of C-furSema and one subunit containing only the 13 N-terminal helical residues (C-furSema^{Het}) (Figure 5A). This construct contains the full N-terminal helix but only a single C-terminal arginine. This unique disulfide-linked heterodimer was produced and purified to >95% purity (Figure 5B). Strikingly, C-furSema^{Het} was as potent as C-furSema at inhibiting VEGF-A-dependent activation of endothelial cells (Figure 5C) and binding of VEGF-A to Nrp1 (Figure 5D; IC_{50} = 35 ± 3 and 24 ± 1 nM, respectively). This is in stark contrast to C-furSema^{Mon}, with an IC_{50} of 1.3 ± 0.7 μM (Figure 5D). These data emphasize the importance of the N-terminal helical region and demonstrate that C-furSema potency is determined by a heterobivalent mechanism combining a C-terminal arginine and structured N-terminal helical region.

Insights into Distinctly Furin-Processed Forms of Sema3A. This raises the question of whether the distance between the C-terminal arginine and helical region is a critical factor in determining Sema3 engagement of Nrp1. There are between one and three furin cleavage sites in the C-terminal basic domain of different Sema3 family members, which produce natural variants with different spacing between the C-terminal arginine and the dimeric helical region. While Sema3F possesses one furin consensus site, Sema3A possesses three. These three sites in Sema3A are known to be processed and important for function[26] (Figure 6). To define the role of the multiple furin processing sites in Sema3A, we measured the inhibitory potency of the three processed variants of Sema3A. The furin-processed forms similar to C-furSema, Sema3A.2 and Sema3A.3, are similar in potency (Figure 6B; IC_{50} values of 45 ± 12 and 27 ± 5 nM, respectively). Intriguingly, the shortest form, Sema3A.1, shows significantly reduced potency (IC_{50} = 1.1 ± 0.3 μM). This form has the same amino acid sequence in both helical and C-terminal motifs, differing only in the spacing of these motifs. These data suggest that furin site selection may represent a natural mechanism for producing Sema3A proteins with differing Nrp binding motif spacing, providing a unique mechanism for fine-tuning Sema3A−Nrp1 binding.

dx.doi.org/10.1021/bi401034q | *Biochemistry* 2013, 52, 7551−7558

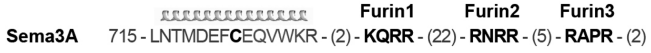

Isoforms	IC_{50}
Sema3A.1	1100 ± 300 nM
Sema3A.2	45 ± 12 nM
Sema3A.3	27 ± 5 nM

Figure 6. Differential furin processing of Sema3A. Sema3A possesses a disulfide-bonded dimeric helical motif followed by three furin consensus (RXXR) sites. These three distinct furin processing sites produce C-terminal domains of significantly different lengths and potencies.

DISCUSSION

Together, these data demonstrate that Sema3 family members engage Nrp1 utilizing two distinct regions in their C-terminal domain, a C-terminal arginine and an upstream helical region. This engagement results in potent competitive binding to Nrp1 that antagonizes VEGF binding and cellular activation. Importantly, the decreased potency observed between dimeric and monomeric forms of C-furSema is primarily due not to the presence of two C-terminal arginine motifs but instead to the presence of the stable helical motif, as demonstrated by the potency of C-furSema^{Het}. These data indicate that the potent competitive binding of C-furSema to Nrp1 is determined by a unique heterobivalent mechanism requiring only one C-terminal arginine and the novel upstream helical region.

Previously, it has been shown that the exon 7-encoded residues of VEGF-A engage loop L1 of the Nrp1-b1 domain, enhancing binding and controlling Nrp1 receptor selectivity.[22] In contrast, loop L1 of Nrp1/2 does not play a role in selective Sema3 binding.[36] Our current data demonstrate that Sema3s utilize their upstream helical motifs to allow potent heterobivalent engagement of Nrp. The physical location of the Sema3 helical binding site on Nrp1 is an important future direction for both mechanistic insights into Sema3 function and inhibitor design. It is notable that Sema3A.1 possesses only four residues between the N-terminal helical region and the C-terminal arginine and has significantly reduced potency, indicating a minimal length is required to tether these two physically distinct sites. Thus, VEGF and Sema3 utilize both common and unique mechanisms to engage Nrp1.

Because Nrp has critical roles in pathological angiogenesis and aberrant axon guidance, significant effort has been devoted to producing Nrp inhibitors. Peptide and small molecule inhibitors have been produced against the C-terminal arginine binding pocket but generally possess modest (micromolar) potency.[28,33,34,37] We demonstrate that by coupling inhibitor oligomerization with covalent tethering of the helical and C-terminal arginine binding motif, we can achieve a two order-of-magnitude increase in inhibitory potency. The identification of two distinct Nrp1 binding sites that, when tethered together, produce a potent inhibitor presents exciting possibilities for fragment-based design strategies combining existing inhibitors of the C-terminal arginine binding pocket with novel helical motif binding site inhibitors.

The physiological role of furin processing in the regulation of Sema3 signaling, as opposed to inhibition of VEGF binding, remains to be determined. While inhibition requires avid binding to only a single Nrp receptor, Sema3 signaling minimally requires the engagement of two receptor molecules and assembly of the signaling complex. Our data indicate that, at a minimum, furin processing is required to activate Sema3 for Nrp-b1 domain binding by liberation of a C-terminal arginine. Importantly, C-furSema^{Het} maintains the potent engagement of Nrp, suggesting that furin processing of a single subunit of the Sema3 dimer may be sufficient for potent activation. Alternatively, furin processing may affect Sema3 engagement of the Nrp-b1 domain quantitatively such that the different forms have progressively increasing signal potency from unprocessed to singly processed to dual processed.

Sema3 engagement of Nrp is more complex than VEGF engagement in that two distinct domains are required. Both binding of the Sema3 C-terminal domain to the Nrp-b1 domain and binding of the Sema3 Sema domain to the Nrp-a1 domain are important for Sema3 signaling.[38,39] Recent structural work has provided significant insight into the contribution of the Nrp-a1 domain in Sema3 binding[40] and assembly of the active Sema3−Plexin−Nrp complex.[41] The specific contribution of a1 and b1 domains in terms of binding potency, specificity, and coupling between the two interacting domains is an active area of research.[6]

The ability of Sema3 to engage the Nrp-b1 domain has clear implications for Sema3 signaling in the nervous system but also in the cardiovascular systems. For example, Sema3A, which is critical for nervous system development,[42] has been shown to inhibit VEGF-dependent angiogenesis yet acts as a vascular permeability factor.[12] Inhibition of VEGF is consistent with our data demonstrating direct competition for Nrp binding. However, induction of vascular permeability by Sema3 was found to be due to specific Nrp-dependent signaling rather than competitive binding. It is possible that these two functions of Sema3 in the cardiovascular systems are differentially regulated by furin processing. Indeed, furin processing of Sema3 family members may have significant physiological implications for regulated function in both nervous and cardiovascular systems.[1]

Our data demonstrate that the furin cleavage sites in the C-terminal domain of Sema3A are nonequivalent in terms of receptor binding. Thus, C-terminal furin processing not only functions as a binary activation mechanism but also can produce activated species with differing physical properties. Recent data indicate that this may have profound physiological implications. Mutations of two different residues in the Sema3A.1 furin site, R730Q and R733H, have recently been shown to cause Kallmann's syndrome, a serious genetic disease resulting from aberrant Sema3A-dependent axon guidance.[43] Thus, differential furin processing of the C-terminal domain of Sema3 can have profound functional and physiological effects in human disease. Combined with these mechanistic insights, the discovery of these disease-associated mutations underlines the importance of future studies of the regulation and function of differential furin processing of Sema3 in regulating Nrp engagement in both neuronal and cardiovascular signaling.

AUTHOR INFORMATION

Corresponding Author

*Address: 741 S. Limestone Ave., BBSRB B263, Lexington, KY 40536. E-mail: craig.vanderkooi@uky.edu. Telephone: (859) 323-8418. Fax: (859) 257-2283.

Present Address

[‖]P.M.B.: Questcor Pharmaceuticals, Ellicott, MD 21043.

Funding

This study was supported by National Institutes of Health Grants R01GM094155 (C.W.V.K.), T32HL072743 (M.W.P.),

and P20GM103486 (core support) and the Kentucky Lung Cancer Research Program.

Notes

The authors declare no competing financial interest.

■ ACKNOWLEDGMENTS

We thank Dr. Matthew Gentry, Dr. David Rodgers, and David Meekins for helpful discussions.

■ ABBREVIATIONS

AP, alkaline phosphatase; HUVECs, human umbilical vein endothelial cells; PAE, porcine aortic endothelial; Nrp1, neuropilin-1; Sema3A–Sema3G, semaphorin 3A–3G, respectively; C-furSema, furin-processed C-terminal domain of Sema3F; VEGF-A, vascular endothelial growth factor-A; VEGFR-2, vascular endothelial growth factor receptor-2; PBS, phosphate-buffered saline; FBS, fetal bovine serum; EBM-2, endothelial cell basal growth medium-2; HRP, horseradish peroxidase; ECL, enhanced chemiluminescence; ELISA, enzyme-linked immunosorbent assay; ECGM, endothelial cell growth medium; IMAC, nickel affinity chromatography; CHO, Chinese hamster ovary; pNPP, *p*-nitrophenol phosphate; HPLC, high-performance liquid chromatography; CD, circular dichroism.

■ REFERENCES

(1) Parker, M. W., Guo, H. F., Li, X., Linkugel, A. D., and Vander Kooi, C. W. (2012) Function of members of the neuropilin family as essential pleiotropic cell surface receptors. *Biochemistry 51*, 9437–9446.

(2) Geretti, E., Shimizu, A., and Klagsbrun, M. (2008) Neuropilin structure governs VEGF and semaphorin binding and regulates angiogenesis. *Angiogenesis 11*, 31–39.

(3) Pellet-Many, C., Frankel, P., Jia, H., and Zachary, I. (2008) Neuropilins: Structure, function and role in disease. *Biochem. J. 411*, 211–226.

(4) de Wit, J., and Verhaagen, J. (2003) Role of semaphorins in the adult nervous system. *Prog. Neurobiol. 71*, 249–267.

(5) Gu, C., and Giraudo, E. (2013) The role of semaphorins and their receptors in vascular development and cancer. *Exp. Cell Res. 319*, 1306–1316.

(6) Hota, P. K., and Buck, M. (2012) Plexin structures are coming: Opportunities for multilevel investigations of semaphorin guidance receptors, their cell signaling mechanisms, and functions. *Cell. Mol. Life Sci. 69*, 3765–3805.

(7) Futamura, M., Kamino, H., Miyamoto, Y., Kitamura, N., Nakamura, Y., Ohnishi, S., Masuda, Y., and Arakawa, H. (2007) Possible role of semaphorin 3F, a candidate tumor suppressor gene at 3p21.3, in p53-regulated tumor angiogenesis suppression. *Cancer Res. 67*, 1451–1460.

(8) Gaur, P., Bielenberg, D. R., Samuel, S., Bose, D., Zhou, Y., Gray, M. J., Dallas, N. A., Fan, F., Xia, L., Lu, J., and Ellis, L. M. (2009) Role of class 3 semaphorins and their receptors in tumor growth and angiogenesis. *Clin. Cancer Res. 15*, 6763–6770.

(9) Joyal, J. S., Sitaras, N., Binet, F., Rivera, J. C., Stahl, A., Zaniolo, K., Shao, Z., Polosa, A., Zhu, T., Hamel, D., Djavari, M., Kunik, D., Honore, J. C., Picard, E., Zabeida, A., Varma, D. R., Hickson, G., Mancini, J., Klagsbrun, M., Costantino, S., Beausejour, C., Lachapelle, P., Smith, L. E., Chemtob, S., and Sapieha, P. (2011) Ischemic neurons prevent vascular regeneration of neural tissue by secreting semaphorin 3A. *Blood 117*, 6024–6035.

(10) Buehler, A., Sitaras, N., Favret, S., Bucher, F., Berger, S., Pielen, A., Joyal, J. S., Juan, A. M., Martin, G., Schlunck, G., Agostini, H. T., Klagsbrun, M., Smith, L. E., Sapieha, P., and Stahl, A. (2013) Semaphorin 3F forms an anti-angiogenic barrier in outer retina. *FEBS Lett. 587*, 1650–1655.

(11) Fukushima, Y., Okada, M., Kataoka, H., Hirashima, M., Yoshida, Y., Mann, F., Gomi, F., Nishida, K., Nishikawa, S., and Uemura, A. (2011) Sema3E-PlexinD1 signaling selectively suppresses disoriented angiogenesis in ischemic retinopathy in mice. *J. Clin. Invest. 121*, 1974–1985.

(12) Acevedo, L. M., Barillas, S., Weis, S. M., Gothert, J. R., and Cheresh, D. A. (2008) Semaphorin 3A suppresses VEGF-mediated angiogenesis yet acts as a vascular permeability factor. *Blood 111*, 2674–2680.

(13) Sekido, Y., Bader, S., Latif, F., Chen, J. Y., Duh, F. M., Wei, M. H., Albanesi, J. P., Lee, C. C., Lerman, M. I., and Minna, J. D. (1996) Human semaphorins A(V) and IV reside in the 3p21.3 small cell lung cancer deletion region and demonstrate distinct expression patterns. *Proc. Natl. Acad. Sci. U.S.A. 93*, 4120–4125.

(14) Capparuccia, L., and Tamagnone, L. (2009) Semaphorin signaling in cancer cells and in cells of the tumor microenvironment: Two sides of a coin. *J. Cell Sci. 122*, 1723–1736.

(15) Potiron, V. A., Roche, J., and Drabkin, H. A. (2009) Semaphorins and their receptors in lung cancer. *Cancer Lett. 273*, 1–14.

(16) Bielenberg, D. R., Hida, Y., Shimizu, A., Kaipainen, A., Kreuter, M., Kim, C. C., and Klagsbrun, M. (2004) Semaphorin 3F, a chemorepulsant for endothelial cells, induces a poorly vascularized, encapsulated, nonmetastatic tumor phenotype. *J. Clin. Invest. 114*, 1260–1271.

(17) Kessler, O., Shraga-Heled, N., Lange, T., Gutmann-Raviv, N., Sabo, E., Baruch, L., Machluf, M., and Neufeld, G. (2004) Semaphorin-3F is an inhibitor of tumor angiogenesis. *Cancer Res. 64*, 1008–1015.

(18) Castro-Rivera, E., Ran, S., Thorpe, P., and Minna, J. D. (2004) Semaphorin 3B (SEMA3B) induces apoptosis in lung and breast cancer, whereas VEGF165 antagonizes this effect. *Proc. Natl. Acad. Sci. U.S.A. 101*, 11432–11437.

(19) Vander Kooi, C. W., Jusino, M. A., Perman, B., Neau, D. B., Bellamy, H. D., and Leahy, D. J. (2007) Structural basis for ligand and heparin binding to neuropilin B domains. *Proc. Natl. Acad. Sci. U.S.A. 104*, 6152–6157.

(20) Parker, M. W., Hellman, L. M., Xu, P., Fried, M. G., and Vander Kooi, C. W. (2010) Furin processing of semaphorin 3F determines its anti-angiogenic activity by regulating direct binding and competition for neuropilin. *Biochemistry 49*, 4068–4075.

(21) Delcombel, R., Janssen, L., Vassy, R., Gammons, M., Haddad, O., Richard, B., Letourneur, D., Bates, D., Hendricks, C., Waltenberger, J., Starzec, A., Sounni, N. E., Noel, A., Deroanne, C., Lambert, C., and Colige, A. (2013) New prospects in the roles of the C-terminal domains of VEGF-A and their cooperation for ligand binding, cellular signaling and vessels formation. *Angiogenesis 16*, 353–371.

(22) Parker, M. W., Xu, P., Li, X., and Vander Kooi, C. W. (2012) Structural basis for the selective vascular endothelial growth factor-A (VEGF-A) binding to neuropilin-1. *J. Biol. Chem. 287*, 11082–11089.

(23) Varshavsky, A., Kessler, O., Abramovitch, S., Kigel, B., Zaffryar, S., Akiri, G., and Neufeld, G. (2008) Semaphorin-3B is an angiogenesis inhibitor that is inactivated by furin-like pro-protein convertases. *Cancer Res. 68*, 6922–6931.

(24) Casazza, A., Kigel, B., Maione, F., Capparuccia, L., Kessler, O., Giraudo, E., Mazzone, M., Neufeld, G., and Tamagnone, L. (2012) Tumour growth inhibition and anti-metastatic activity of a mutated furin-resistant Semaphorin 3E isoform. *EMBO Mol. Med. 4*, 234–250.

(25) Christensen, C., Ambartsumian, N., Gilestro, G., Thomsen, B., Comoglio, P., Tamagnone, L., Guldberg, P., and Lukanidin, E. (2005) Proteolytic processing converts the repelling signal Sema3E into an inducer of invasive growth and lung metastasis. *Cancer Res. 65*, 6167–6177.

(26) Adams, R. H., Lohrum, M., Klostermann, A., Betz, H., and Puschel, A. W. (1997) The chemorepulsive activity of secreted semaphorins is regulated by furin-dependent proteolytic processing. *EMBO J. 16*, 6077–6086.

(27) Starzec, A., Vassy, R., Martin, A., Lecouvey, M., Di Benedetto, M., Crepin, M., and Perret, G. Y. (2006) Antiangiogenic and antitumor

activities of peptide inhibiting the vascular endothelial growth factor binding to neuropilin-1. *Life Sci. 79*, 2370−2381.
(28) von Wronski, M. A., Raju, N., Pillai, R., Bogdan, N. J., Marinelli, E. R., Nanjappan, P., Ramalingam, K., Arunachalam, T., Eaton, S., Linder, K. E., Yan, F., Pochon, S., Tweedle, M. F., and Nunn, A. D. (2006) Tuftsin binds neuropilin-1 through a sequence similar to that encoded by exon 8 of vascular endothelial growth factor. *J. Biol. Chem. 281*, 5702−5710.
(29) Teesalu, T., Sugahara, K. N., Kotamraju, V. R., and Ruoslahti, E. (2009) C-end rule peptides mediate neuropilin-1-dependent cell, vascular, and tissue penetration. *Proc. Natl. Acad. Sci. U.S.A. 106*, 16157−16162.
(30) Becker, P. M., Waltenberger, J., Yachechko, R., Mirzapoiazova, T., Sham, J. S., Lee, C. G., Elias, J. A., and Verin, A. D. (2005) Neuropilin-1 regulates vascular endothelial growth factor-mediated endothelial permeability. *Circ. Res. 96*, 1257−1265.
(31) Jardin, B. A., Zhao, Y., Selvaraj, M., Montes, J., Tran, R., Prakash, S., and Elias, C. B. (2008) Expression of SEAP (secreted alkaline phosphatase) by baculovirus mediated transduction of HEK 293 cells in a hollow fiber bioreactor system. *J. Biotechnol. 135*, 272−280.
(32) Louis-Jeune, C., Andrade-Navarro, M. A., and Perez-Iratxeta, C. (2012) Prediction of protein secondary structure from circular dichroism using theoretically derived spectra. *Proteins: Struct., Funct., Bioinf. 80*, 374−381.
(33) Jarvis, A., Allerston, C. K., Jia, H., Herzog, B., Garza-Garcia, A., Winfield, N., Ellard, K., Aqil, R., Lynch, R., Chapman, C., Hartzoulakis, B., Nally, J., Stewart, M., Cheng, L., Menon, M., Tickner, M., Djordjevic, S., Driscoll, P. C., Zachary, I., and Selwood, D. L. (2010) Small molecule inhibitors of the neuropilin-1 vascular endothelial growth factor A (VEGF-A) interaction. *J. Med. Chem. 53*, 2215−2226.
(34) Jia, H., Bagherzadeh, A., Hartzoulakis, B., Jarvis, A., Lohr, M., Shaikh, S., Aqil, R., Cheng, L., Tickner, M., Esposito, D., Harris, R., Driscoll, P. C., Selwood, D. L., and Zachary, I. C. (2006) Characterization of a bicyclic peptide neuropilin-1 (NP-1) antagonist (EG3287) reveals importance of vascular endothelial growth factor exon 8 for NP-1 binding and role of NP-1 in KDR signaling. *J. Biol. Chem. 281*, 13493−13502.
(35) Parker, M. W., Linkugel, A. D., and Vander Kooi, C. W. (2013) Effect of C-terminal Sequence on Competitive Semaphorin Binding to Neuropilin-1. *J. Mol. Biol.*, DOI: 10.1016/j.jmb.2013.07.017.
(36) Parker, M. W., Xu, P., Guo, H. F., and Vander Kooi, C. W. (2012) Mechanism of selective VEGF-A binding by neuropilin-1 reveals a basis for specific ligand inhibition. *PLoS One 7*, e49177.
(37) Binetruy-Tournaire, R., Demangel, C., Malavaud, B., Vassy, R., Rouyre, S., Kraemer, M., Plouet, J., Derbin, C., Perret, G., and Mazie, J. C. (2000) Identification of a peptide blocking vascular endothelial growth factor (VEGF)-mediated angiogenesis. *EMBO J. 19*, 1525−1533.
(38) Gu, C., Limberg, B. J., Whitaker, G. B., Perman, B., Leahy, D. J., Rosenbaum, J. S., Ginty, D. D., and Kolodkin, A. L. (2002) Characterization of neuropilin-1 structural features that confer binding to semaphorin 3A and vascular endothelial growth factor 165. *J. Biol. Chem. 277*, 18069−18076.
(39) Koppel, A. M., Feiner, L., Kobayashi, H., and Raper, J. A. (1997) A 70 amino acid region within the semaphorin domain activates specific cellular response of semaphorin family members. *Neuron 19*, 531−537.
(40) Appleton, B. A., Wu, P., Maloney, J., Yin, J., Liang, W. C., Stawicki, S., Mortara, K., Bowman, K. K., Elliott, J. M., Desmarais, W., Bazan, J. F., Bagri, A., Tessier-Lavigne, M., Koch, A. W., Wu, Y., Watts, R. J., and Wiesmann, C. (2007) Structural studies of neuropilin/antibody complexes provide insights into semaphorin and VEGF binding. *EMBO J. 26*, 4902−4912.
(41) Janssen, B. J., Malinauskas, T., Weir, G. A., Cader, M. Z., Siebold, C., and Jones, E. Y. (2012) Neuropilins lock secreted semaphorins onto plexins in a ternary signaling complex. *Nat. Struct. Mol. Biol. 19*, 1293−1299.
(42) Pasterkamp, R. J. (2012) Getting neural circuits into shape with semaphorins. *Nat. Rev. Neurosci. 13*, 605−618.
(43) Hanchate, N. K., Giacobini, P., Lhuillier, P., Parkash, J., Espy, C., Fouveaut, C., Leroy, C., Baron, S., Campagne, C., Vanacker, C., Collier, F., Cruaud, C., Meyer, V., Garcia-Pinero, A., Dewailly, D., Cortet-Rudelli, C., Gersak, K., Metz, C., Chabrier, G., Pugeat, M., Young, J., Hardelin, J. P., Prevot, V., and Dode, C. (2012) SEMA3A, a gene involved in axonal pathfinding, is mutated in patients with Kallmann syndrome. *PLoS Genet. 8*, e1002896.